Frontiers of Information Technology & Electronic Engineering
www.jzus.zju.edu.cn; engineering.cae.cn; www.springerlink.com
ISSN 2095-9184 (print); ISSN 2095-9230 (online)
E-mail: jzus@zju.edu.cn

Synchronization of nonlinear multi-agent systems using a non-fragile sampled data control approach and its application to circuit systems*

Stephen AROCKIA SAMY[1], Raja RAMACHANDRAN[2], Pratap ANBALAGAN[3], Yang CAO[†‡4]

[1]*Department of Mathematics, Alagappa University, Karaikudi 630 003, Tamil Nadu, India*

[2]*Ramanujan Centre for Higher Mathematics, Alagappa University, Karaikudi 630 003, Tamil Nadu, India*

[3]*Research Center for Wind Energy Systems, Kunsan National University, Gunsan 573-701, Republic of Korea*

[4]*School of Cyber Science and Engineering, Southeast University, Nanjing 210096, China*

[†]E-mail: caoyeacy@seu.edu.cn

Received Apr. 30, 2022; Revision accepted Aug. 24, 2022; Crosschecked Mar. 27, 2023

Abstract: The main aim of this work is to design a non-fragile sampled data control (NFSDC) scheme for the asymptotic synchronization criteria for interconnected coupled circuit systems (multi-agent systems, MASs). NFSDC is used to conduct synchronization analysis of the considered MASs in the presence of time-varying delays. By constructing suitable Lyapunov functions, sufficient conditions are derived in terms of linear matrix inequalities (LMIs) to ensure synchronization between the MAS leader and follower systems. Finally, two numerical examples are given to show the effectiveness of the proposed control scheme and less conservation of the proposed Lyapunov functions.

Key words: Multi-agent systems (MASs); Non-fragile sampled data control (NFSDC); Time-varying delay; Linear matrix inequality (LMI); Asymptotic synchronization

https://doi.org/10.1631/FITEE.2200181 **CLC number:** TP13

1 Introduction

In recent times, multi-agent systems (MASs) have emerged as the most important nonlinear model and have been used efficiently (Beard et al., 2002; Fax and Murray, 2004; Ren and Sorensen, 2008). A system is composed of small subsystems, known as agents, which work together to form a network of other agents. Agents can connect with one another through a network to accomplish global objectives without the need of local contact or supervisors. Acquiring data from all agents is a challenging task, even though the entire system is controlled. In such cases, we use a multichannel system view. Specifically, in agreement with the prearranged values of our problem, data acquisition can be categorized as a leader-follower (Jia et al., 2011; Rakkiyappan et al., 2015; Tang et al., 2015) or a leaderless problem (Meng et al., 2011). In the leader-follower problem, the leader serves as a commander, who creates the necessary path without the knowledge of the followers. A subgroup of followers must directly access the information about the leader in this case. For some applications, MAS integration is not a single phase, but rather a two-part process that includes a balancing physical and communication restrictions. In this context, the research on MASs has progressed dramatically in recent years (Wang CY et al., 2019; Liu JL et al., 2021; Yue et al., 2021).

‡ Corresponding author

* Project supported by the National Natural Science Foundation of China (No. 62103103) and the Natural Science Foundation of Jiangsu Province, China (No. BK20210223)

ORCID: Stephen AROCKIA SAMY, https://orcid.org/0000-0001-9040-556X; Yang CAO, https://orcid.org/0000-0002-6940-0868

Artificial neural networks (ANNs) have grown in popularity among the scientists and researchers who worked in the field of artificial intelligence networks since the 1980s. A neural network (NN) is a computer imitation composed of nodes that are connected to each other (or neurons). ANN research has made major progress in biology, automatic control, computer acknowledgement, etc., providing a better understanding of challenging and practical issues of modern systems (Sompolinsky et al., 1988; Chen and Aihara, 1995; Zheng et al., 2017). In this regard, ANNs provide substantial nonlinearities, making it challenging to analyze their dynamical properties. Thus, several researchers have focused their efforts on analyzing the dynamical behavior of ANNs and have produced some noticeable results in Alimi et al. (2019) and Wang WP et al. (2019).

In practice, chaotic synchronization is a critical matter in nonlinear science. The concept of chaotic synchronization involves synchronizing two chaotic systems. However, the projected results indicated that the followers' system actions had an effect on the leader system, despite the fact that the leader system was self-contained. The fundamental complexity of nonlinear dynamics causes extra challenges in handling synchronization issues in MASs in this paper. Note that the aforementioned literature primarily focused on synchronized MASs, in which all agents have similar dynamics. However, in real-world applications, various dynamics may be more realistic. As a result, studying synchronization in MASs becomes significantly more difficult. A practical synchronization is used in this case because of many different types of agents in the system. Indeed, MAS synchronization issues are difficult to tackle due to the intrinsic complexity of nonlinear dynamics. Jia et al. (2019) addressed synchronization of MASs with time-varying control and delayed communications. Sang and Zhao (2019) studied the chaotic synchronization for NNs under time-varying delays using the Lyapunov stability theory. Kaviarasan et al. (2021) investigated a stochastic non-fragile controller for MASs with a communication delay. In Zhao YS et al. (2019), a widespread synchronization for chaotic NNs was given, and numerous suitable conditions were found by employing a suitable Lyapunov-Krosovskii functional.

To achieve the MAS aim, many control systems have been used, including impulsive control, event-triggered control (Zhou et al., 2015), pinning control (Wang YL et al., 2014), quantized control (Tan et al., 2019), and adaptive control. Zhang et al. (2018) and Jiang et al. (2020) derived sampled data control (SDC) for MASs. Zhong et al. (2022) discussed H_∞ load frequency control for a multi-area power system based on non-fragile propositional integral control. Among them, SDC performed well in a task to study the dynamics of MASs due to the improvement of digital technology. The main purpose of SDC is to update the control signals only at sampling instants during the sampling intervals. In sampling intervals, control signals on SDC systems are consistent and may change only during the instants of the sample. Control signals are thus gradually transmitted in SDC systems, and these discontinuous signals cannot be employed directly for stabilizing the control systems. From this perspective, SDC has been increasingly important in control systems, and some remarkable results have been achieved (Liu Y et al., 2019; Xu et al., 2021; Zhao C et al., 2021; Lavanya and Nagarani, 2022). On the other hand, non-fragile control can adjust gain fluctuation in the design of the controller and is used to assure system stability when small disruptions occur in the design of the controller. A few noteworthy works on the non-fragile control problem in MASs have been published (Ali et al., 2020b; Saravanakumar et al., 2020).

To a greater extent, the conditions for achieving asymptotic synchronization of nonlinear MASs with non-fragile sampled data control (NFSDC) have not been comprehensively addressed (Zhang et al., 2018; Jia et al., 2019; Jiang et al., 2020), which serves as a motivation for the investigation in this paper.

The contributions of this paper are summarized as follows:

1. In practical applications, NN-based circuit systems are modeled as MAS-based leader and follower systems for analyzing the synchronization issue, which is based on Lyapunov-Krasovskii functional with Kronecker product.

2. For MASs, NFSDC is designed, and then sufficient conditions of synchronization criteria are derived using Lemma 1. The derived conditions assure the asymptotic stability of the MAS error system of MASs.

3. The generality of our strategy for designing a controller distinguishes it from the past work in this area of research. Furthermore, it provides a broad

framework for investigating synchronization difficulties that are related to the consistency of control strength over time, such as NFSDC.

4. The approaches in Ma et al. (2016) have been compared to confirm the efficacy of the suggested method in the numerical simulation.

According to Theorem 2, designing NFSDC can achieve leader-following synchronization of MASs with time-varying delay. Some improved inequality techniques have been successfully used for MASs. As a result, the whole analysis procedure has been simplified. Furthermore, less conservative stability requirements are constructed using linear matrix inequalities (LMIs). Finally, numerical validation confirms the effectiveness of the designed control strategy using MASs, indicating the efficacy of our suggested method when time-varying delays occur.

Notations: $\mathbb{R}^n$ and $\mathbb{R}^{n\times n}$ denote the n-dimensional Euclidean space and $n\times n$ real matrices, respectively. 0 and I refer to the zero and identity matrices with suitable dimensions, respectively. Superscript T denotes the transpose of a matrix. $\otimes$ refers to the Kronecker product. $\|\cdot\|$ refers the Euclidean norm of a vector.

2 Problem statement and preliminaries

This section provides the preliminary work for our main study, including some fundamental concepts in algebraic graph theory and mathematical representations of the relevant subject.

Let $G=(\nu,\varepsilon,\mathcal{W})$ be an interconnection graph that is used to connect N agents, each of which has a node $\nu=\{z_1,z_2,\cdots,z_N\}$ and a directed edge $\varepsilon\subseteq\{\nu\times\nu\}$. If the edge $(z_i,z_j)\in\varepsilon$ from agent z_j to z_i, then z_j is a neighbor of z_i and $\mathcal{W}=[a_{ij}]_{N\times N}$ is the adjacent weighted matrix. The edge of agent z_i to z_j is a_{ij} and must be zero. N_i denotes the set of agent neighbors i. A path of agent z_j toward agent z_i is a string sequence of edges $(z_i,z_{l_1}),(z_{l_1},z_{l_2}),\cdots,(z_{l_m},z_j)$. When a directional path from one node to the other node exists, the directional graph is said to be strongly linked. The Laplacian matrix $L=(l_{ij})_{N\times N}$ of G is defined by $l_{ij}=-a_{ij}$, $i\neq j$, $l_{ii}=\sum_{j=1,j\neq i}^{N}a_{ij}$ $(i,j=1,2,\cdots,N)$.

Let us consider the leader and followers system as follows:

$$\begin{cases}\text{Leader :}\\ \dot{z}_0(t)=-Az_0(t)+Bg(z_0(t))+Cg(z_0(t-\iota(t))),\\ \text{Followers :}\\ \dot{z}_i(t)=-Az_i(t)+Bg(z_i(t))+Cg(z_i(t-\iota(t)))\\ \qquad\quad +U(t),\end{cases}\tag{1}$$

where $z_0(t)=[z_{01}(t),\ z_{02}(t),\ ...,\ z_{0n}(t)]^{\mathrm{T}}\in\mathbb{R}^n$ refers to the state of the leader agents, and $z_i(t)=[z_{i1}(t),\ z_{i2}(t),\ ...,\ z_{in}(t)]^{\mathrm{T}}\in\mathbb{R}^n$ refers to the state of the i^{th} agent. The control input is $u_i(t)\in\mathbb{R}^n$. $A=\mathrm{diag}(a_1,\ a_2,\ ....,a_n)$ is a diagonal matrix, and $B=(b_{ij})_{n\times n}$ and $C=(c_{ij})_{n\times n}$ are weight matrices. $g(z_0(t))$ and $g(z_i(t))\in\mathbb{R}^n$ represent the activation functions of the leader system and follower system, respectively. $\iota(t)$ is a time-varying delay and satisfies $0\leq\iota(t)<\iota$ and $i(t)\leq\lambda$, where $\lambda>0$ and $\iota>0$ are constants.

Here, cooperative synchronization implies that the two dynamic systems with the leader and followers will attain the same partial state simultaneously. Generally, the leader uses channels to broadcast a communication signal that triggers the followers, and this signal induces the coordination between the leader and followers.

Let $\eta_i(t)=z_i(t)-z_0(t)$. The synchronization error is described as

$$\begin{aligned}\dot{\eta}_i(t)=&-A\eta_i(t)+Bh(\eta_i(t))\\&+Ch(\eta_i(t-\iota(t)))+u_i(t).\end{aligned}\tag{2}$$

The compact representation of the synchronization error system (2) is given below:

$$\begin{aligned}\dot{\eta}(t)=&-(I\otimes A)\eta(t)+(I\otimes B)h(\eta(t))\\&+(I\otimes C)h(\eta(t-\iota(t)))+U(t),\end{aligned}\tag{3}$$

where $\eta(t)=[\eta_1(t),\eta_2(t),\cdots,\eta_N(t)]^{\mathrm{T}}$, $U(t)=[u_1(t),u_2(t),\cdots,u_N(t)]^{\mathrm{T}}$, $h(\eta(t))=[g(\eta_1(t))-g(\eta_0(t)),g(\eta_2(t))-g(\eta_0(t)),\cdots,g(\eta_N(t))-g(\eta_0(t))]^{\mathrm{T}}$, and $h(\eta(t-\iota(t)))=[g(\eta_1(t-\iota(t)))-g(\eta_0(t-\iota(t))),g(\eta_2(t-\iota(t)))-g(\eta_0(t-\iota(t))),\cdots,g(\eta_N(t-\iota(t)))-g(\eta_0(t-\iota(t)))]^{\mathrm{T}}$.

Definition 1 (Subramanian et al., 2019) The MAS (1) is called asymptotic synchronization if

$$\lim_{t\to\infty}\|\eta_i(t)\|=\lim_{t\to\infty}\|z_i(t)-z_0(t)\|=0,$$

for all $i=1,2,\cdots,N$.

It is possible to obtain sufficient conditions with a suitable Lyapunov function using the following lemma:

Lemma 1 (Seuret and Gouaisbaut, 2013) For a given matrix $\bar{Q} > 0$, the following inequality holds for $\omega : [c, d] \to \mathbb{R}^n$:

$$-\int_c^d \dot{\omega}^{\mathrm{T}}(\varsigma)\bar{Q}\dot{\omega}(\varsigma)\mathrm{d}\varsigma \le -\frac{1}{d-c}(\omega(d)-\omega(c))^{\mathrm{T}}\bar{Q} \cdot (\omega(d)-\omega(c)) - \frac{3}{d-c}\Pi^{\mathrm{T}}\bar{Q}\Pi,$$

where $\Pi = \omega(d) + \omega(c) - \frac{2}{d-c}\int_c^d \omega(\varsigma)\mathrm{d}\varsigma$.

Assumption 1 (Ali et al., 2020a) For all $q = 1, 2, \cdots, n$ and $g_q(\cdot)$, there exist positive constants Θ_q^- and Θ_q^+ such that

$$\Theta_q^- \le \frac{g_q(a)-g_q(b)}{a-b} \le \Theta_q^+, \ \forall\, a \ne b \in \mathbb{R}.$$

The time-step sampled data from agent i are encapsulated in a packet of data, subsequently transferred to its controller and agent j over agent i communication network. Zero-order hold (ZOH) is used to update the input and output actuators of controller i. ZOH represents the outcome of keeping each sample value for one sample interval while converting a discrete-time signal to a continuous-time signal. Now, we consider the following NFSDC scheme:

$$u_i(t) = \delta(J+\Delta J(t))\Big\{\sum_{j=1}^{N} a_{ij}(z_j(t_k)-z_i(t_k)) - \phi_i(z_i(t_k)-z_0(t_k))\Big\}, \tag{4}$$

where $\delta > 0$ is the coupling strength, J is the feedback controller, and $\Delta J(t)$ is an unknown gain matrix that satisfies $\Delta J = \beta_1\Psi(t)\beta_2$, with $\Psi^{\mathrm{T}}(t)\Psi(t) \le I$, where β_1 and β_2 are two given constant matrices.

To stabilize Eq. (4), we assume that the control has discrete measurements $z(t_k)$ only at sampling instant t_k with $0 = t_0 < t_1 < \cdots < t_k < \cdots < \lim_{k\to\infty} t_k < \infty$. Now, we consider $t_{k+1} - t = \varrho_k < \varrho$, for all $k \ge 0$. Under sampling control, we have $z(t_k) = z(t-\varrho(t))$, where $\varrho(t) = t - t_k$ for $t \in [t_k,\ t_{k+1})$. Then, Eq. (4) can be rewritten as

$$u_i(t) = \delta(J+\Delta J(t))\Big\{-\sum_{j=1}^{N} l_{ij}(z_j(t-\varrho(t)) - z_i(t-\varrho(t))) - \phi_i\eta_i(t-\varrho(t))\Big\}. \tag{5}$$

Define $\Upsilon = \mathrm{diag}(\phi_1, \phi_2, \cdots, \phi_N)$. Then the compact form of NFSDC can be converted into

$$\begin{aligned} U(t) =& -\delta(L\otimes(J+\beta_1\psi(t)\beta_2))(\eta(t-\varrho(t))) \\ & -\delta(\Upsilon\otimes(J+\beta_1\psi(t)\beta_2))(\eta(t-\varrho(t))). \end{aligned} \tag{6}$$

Combining Eqs. (3) and (6), the error system is described as

$$\begin{aligned} \dot{\eta}(t) =& -(I\otimes A)\eta(t) + (I\otimes B)h(\eta(t)) \\ & +(I\otimes C)h(\eta(t-\iota(t))) \\ & -\delta(L\otimes(J+\beta_1\psi(t)\beta_2))(\eta(t-\varrho(t))) \\ & -\delta(\Upsilon\otimes(J+\beta_1\psi(t)\beta_2))(\eta(t-\varrho(t))). \end{aligned} \tag{7}$$

The primary goal of this research is to achieve the asymptotic synchronization of MAS (7) using NFSDC with a large upper sampling interval bound, which is detailed as follows:

Problem 1 Here, the objective is to achieve synchronization between leader and follower systems:

1. We construct the delay-dependent sufficient conditions in the form of LMIs, which demonstrate that multi-agent error dynamic networks (7) can achieve asymptotic synchronization.

2. To solve the LMIs in the appropriate direction, the control gain matrix J is calculated.

3 Main results

The leader-following synchronization of MAS (1) connected by nodes in a topology is discussed in this section.

Theorem 1 Under Assumption 1, for some positive constants ι, λ, ϱ and given gain matrix J, if there exist positive matrices P_1, P_2, P_3, P_4, P_5, P_6, P_7, and any matrices S_1, S_2, and S_3 with appropriate dimensions, such that the following equalities

$$\begin{aligned} \Xi_{11} =& (I\otimes P_2)+(I\otimes P_3)+(I\otimes P_4)-4(I\otimes P_6) \\ & -4(I\otimes P_7)-2(I\otimes S_1A)-\Theta_1(I\otimes M_1) \\ & -\delta^2(L\otimes S_1\beta_1\beta_1^{\mathrm{T}}S_1^{\mathrm{T}})-\delta^2(\Upsilon\otimes S_1\beta_1\beta_1^{\mathrm{T}}S_1^{\mathrm{T}}), \\ \Xi_{12} =& -2(I\otimes P_6), \\ \Xi_{14} =& -(I\otimes S_1A)-\delta(L\otimes S_1J)-\delta(\Upsilon\otimes S_1J), \\ \Xi_{15} =& -2(I\otimes P_7), \\ \Xi_{16} =& -(I\otimes S_1)-(I\otimes S_1A)+(I\otimes P_1), \\ \Xi_{17} =& (I\otimes S_1B)+\Theta_2(I\otimes M_1), \\ \Xi_{18} =& I\otimes S_1C, \end{aligned}$$

$$
\begin{aligned}
&\Xi_{19}=6(I\otimes P_6),\\
&\Xi_{1,10}=6(I\otimes P_7),\\
&\Xi_{22}=-(I\otimes P_3)-4(I\otimes P_6),\\
&\Xi_{29}=6(I\otimes P_6),\\
&\Xi_{33}=-(1-\lambda)(I\otimes P_2)-\Theta_1(I\otimes M_2)\\
&\qquad-\delta^2(L\otimes\beta_1\beta_1^{\mathrm{T}}),\\
&\Xi_{34}=-\delta(L\otimes S_3J)-\delta(\Upsilon\otimes S_3J),\\
&\Xi_{38}=\Theta_2(I\otimes M_2),\\
&\Xi_{44}=-3(L\otimes\beta_2\beta_2^{\mathrm{T}})-3(\Upsilon\otimes\beta_2\beta_2^{\mathrm{T}}),\\
&\Xi_{46}=-(I\otimes\kappa_2S^{\mathrm{T}})-\delta(L\otimes S_1J)-\delta(\Upsilon\otimes S_1J),\\
&\Xi_{47}=I\otimes S_2B,\\
&\Xi_{48}=I\otimes S_3C,\\
&\Xi_{55}=-(I\otimes P_4)-4(I\otimes P_7),\\
&\Xi_{5,10}=6(I\otimes P_7),\\
&\Xi_{66}=\iota^2(I\otimes P_6)+\varrho^2(I\otimes P_7)-2(I\otimes S_2)\\
&\qquad-\delta^2(L\otimes S_2\beta_1\beta_1^{\mathrm{T}}S_2^{\mathrm{T}})-\delta^2(\Upsilon\otimes S_2\beta_1\beta_1^{\mathrm{T}}S_2^{\mathrm{T}}),\\
&\Xi_{67}=(I\otimes S_2B),\\
&\Xi_{68}=I\otimes S_3C,\\
&\Xi_{77}=(I\otimes P_5)-(I\otimes M_1),\\
&\Xi_{88}=-(1-\lambda)(I\otimes P_5)-(I\otimes M_2),\\
&\Xi_{99}=-12(I\otimes P_6),\\
&\Xi_{10,10}=-12(I\otimes P_7),
\end{aligned}
$$

hold for

$$\Xi=[\Xi_{r\kappa}]<0,\ \text{where}\ r,\ \kappa=1,2,\cdots,10, \tag{8}$$

then the considered leader and followers are asymptotically synchronized under the proposed NFSDC scheme (6).

Proof Construct the Lyapunov-Krosovskii functional as follows:

$$V(t)=\sum_{i=1}^{5}V_i(t),\ t\in[t_k,\ t_{k+1}),$$

where

$$
\begin{cases}
V_1(t)=\eta^{\mathrm{T}}(t)(I\otimes P_1)\eta(t),\\
V_2(t)=\int_{t-\iota(t)}^{t}\eta^{\mathrm{T}}(s)(I\otimes P_2)\eta(s)\mathrm{d}s\\
\qquad\quad+\int_{t-\iota}^{t}\eta^{\mathrm{T}}(s)(I\otimes P_3)\eta(s)\mathrm{d}s,\\
V_3(t)=\int_{t-\varrho}^{t}\eta^{\mathrm{T}}(s)(I\otimes P_4)\eta(s)\mathrm{d}s,\\
V_4(t)=\int_{t-\iota(t)}^{t}h^{\mathrm{T}}(\eta(s))(I\otimes P_5)h(\eta(s))\mathrm{d}s,\\
V_5(t)=\iota\int_{t-\iota}^{t}\int_{\theta}^{t}\dot\eta(s)^{\mathrm{T}}(I\otimes P_6)\dot\eta(s)\mathrm{d}s\mathrm{d}\theta\\
\qquad\quad+\varrho\int_{t-\varrho}^{t}\int_{\theta}^{t}\dot\eta(s)^{\mathrm{T}}(I\otimes P_7)\dot\eta(s)\mathrm{d}s\mathrm{d}\theta.
\end{cases}
\tag{9}
$$

Based on Eq. (9), we have

$$
\begin{aligned}
\dot V_1(t)&=2\eta^{\mathrm{T}}(t)(I\otimes P_1)\dot\eta(t)\\
&=\eta^{\mathrm{T}}(t)(I\otimes P_1)\dot\eta(t)+\eta^{\mathrm{T}}(t)(I\otimes P_1)\dot\eta(t),
\end{aligned}
\tag{10}
$$

$$
\begin{aligned}
\dot V_2(t)&=\eta^{\mathrm{T}}(t)(I\otimes P_2)\eta(t)\\
&\quad-(1-\lambda)\eta^{\mathrm{T}}(t-\iota(t))(I\otimes P_2)\eta(t-\iota(t))\\
&\quad+\eta^{\mathrm{T}}(t)(I\otimes P_3)\eta(t)\\
&\quad-\eta^{\mathrm{T}}(t-\iota)(I\otimes P_3)\eta(t-\iota),
\end{aligned}
\tag{11}
$$

$$
\begin{aligned}
\dot V_3(t)=&\eta^{\mathrm{T}}(t)(I\otimes P_4)\eta(t)\\
&-\eta^{\mathrm{T}}(t-\varrho)(I\otimes P_4)\eta(t-\varrho),
\end{aligned}
\tag{12}
$$

$$
\begin{aligned}
\dot V_4(t)&=h^{\mathrm{T}}(\eta(t))(I\otimes P_5)h(\eta(t))\\
&\quad-(1-\dot\iota(t))h^{\mathrm{T}}(\eta(t-\iota(t)))(I\otimes P_5)h(\eta(t-\iota(t)))\\
&\le h^{\mathrm{T}}(\eta(t))(I\otimes P_5)h(\eta(t))\\
&\quad-(1-\lambda)h^{\mathrm{T}}(\eta(t-\iota(t)))(I\otimes P_5)h(\eta(t-\iota(t))),
\end{aligned}
\tag{13}
$$

$$
\begin{aligned}
\dot V_5(t)&=\dot\eta^{\mathrm{T}}(t)\iota^2(I\otimes P_6)\dot\eta(t)\\
&\quad-\iota\int_{t-\iota}^{t}\dot\eta^{\mathrm{T}}(s)(I\otimes P_6)\dot\eta^{\mathrm{T}}(s)\mathrm{d}s\\
&\quad+\dot\eta^{\mathrm{T}}(t)\varrho^2(I\otimes P_7)\dot\eta(t)\\
&\quad-\varrho\int_{t-\varrho}^{t}\dot\eta^{\mathrm{T}}(s)(I\otimes P_7)\dot\eta(s)\mathrm{d}s.
\end{aligned}
\tag{14}
$$

Using Lemma 1, we have

$$
\begin{aligned}
&-\iota\int_{t-\iota}^{t}\dot\eta^{\mathrm{T}}(s)(I\otimes P_6)\dot\eta(s)\mathrm{d}s\\
&\le-[\eta(t)-\eta(t-\iota)]^{\mathrm{T}}(I\otimes P_6)[\eta(t)-\eta(t-\iota)]\\
&\quad-3[\Pi^{\mathrm{T}}(I\otimes P_6)\Pi],
\end{aligned}
\tag{15}
$$

$$
\begin{aligned}
&-\varrho\int_{t-\varrho}^{t}\dot\eta^{\mathrm{T}}(s)(I\otimes P_7)\dot\eta(s)\mathrm{d}s\\
&\le-[\eta(t)-\eta(t-\varrho)]^{\mathrm{T}}(I\otimes P_7)[\eta(t)-\eta(t-\varrho)]\\
&\quad-3[\Pi^{\mathrm{T}}(I\otimes P_7)\Pi].
\end{aligned}
\tag{16}
$$

For any matrices M_1 and M_2, from Assumption 1, we have

$$
\begin{bmatrix}\eta(t)\\ h(\eta(t))\end{bmatrix}^{\mathrm{T}}\begin{bmatrix}-\Theta_1(I\otimes M_1) & \Theta_2(I\otimes M_1)\\ \star & -(I\otimes M_1)\end{bmatrix}\cdot\begin{bmatrix}\eta(t)\\ h(\eta(t))\end{bmatrix}\ge 0.
\tag{17}
$$

$$\begin{bmatrix} \eta(t-\iota(t)) \\ h(\eta(t-\iota(t))) \end{bmatrix}^{\mathrm{T}} \begin{bmatrix} -\Theta_1(I\otimes M_2) & \Theta_2(I\otimes M_2) \\ \star & -(I\otimes M_2) \end{bmatrix} \cdot \begin{bmatrix} \eta(t-\iota(t)) \\ h(\eta(t-\iota(t))) \end{bmatrix} \geq 0. \tag{18}$$

Moreover, for any matrices S_1, S_2, and S_3, it follows that

$$\begin{aligned} 0 =& 2(\eta^{\mathrm{T}}(t)(I\otimes S_1)+\dot{\eta}^{\mathrm{T}}(t)(I\otimes S_2) \\ &+\eta^{\mathrm{T}}(t-\iota(t))(I\otimes S_3))(-\dot{\eta}(t)+\dot{\eta}(t)). \end{aligned} \tag{19}$$

Directly, we denote

$$\vartheta_1=\frac{1}{\iota}\int_{t-\iota}^{t}\eta(s)\mathrm{d}s,\ \vartheta_2=\frac{1}{\varrho}\int_{t-\varrho}^{t}\eta(s)\mathrm{d}s.$$

Hence, on collecting Eqs. (10)–(19), we have

$$\dot{V}(t)\leq\zeta^{\mathrm{T}}(t)\Xi\zeta(t), \tag{20}$$

where

$$\begin{aligned} \zeta^{\mathrm{T}}(t)=\big[&\eta^{\mathrm{T}}(t),\ \eta^{\mathrm{T}}(t-\iota),\ \eta^{\mathrm{T}}(t-\iota(t)),\ \eta^{\mathrm{T}}(t-\varrho(t)), \\ &\eta^{\mathrm{T}}(t-\varrho),\ \dot{\eta}^{\mathrm{T}}(t),\ h^{\mathrm{T}}(\eta(t)),\ h^{\mathrm{T}}(\eta(t-\iota(t))), \\ &\vartheta_1^{\mathrm{T}},\ \vartheta_2^{\mathrm{T}}\big], \end{aligned}$$

and Ξ is as expressed in Theorem 1. If $\Xi<0$, in light of Eq. (8), we have $\dot{V}(t)<0$. This means that, based on the Lyapunov-Krosovskii stability theorem, it is established that the addressed MAS (1) with gain J is asymptotically synchronized. Thus, the proof is completed.

Using Theorem 1, the following Theorem 2 is derived to obtain the control gain matrix for the NFSDC scheme (6) to asymptotically synchronize the leader and followers system (1):

Theorem 2 Under Assumption 1, for some positive constants ι, λ, ϱ, κ_1, and κ_2, if there exist positive matrices $\check{P}_1$, $\check{P}_2$, $\check{P}_3$, $\check{P}_4$, $\check{P}_5$, $\check{P}_6$, $\check{P}_7$, and any matrix S with appropriate dimensions, such that the following equalities

$$\begin{aligned} \check{\Xi}_{11} =&(I\otimes\check{P}_2)+(I\otimes\check{P}_3)+(I\otimes\check{P}_4)-4(I\otimes\check{P}_6) \\ &-4(I\otimes\check{P}_7)-2(I\otimes AS^{\mathrm{T}})-\Theta_1(I\otimes\check{M}_1) \\ &-\delta^2(L\otimes\beta_1\beta_1^{\mathrm{T}})-\delta^2(\Upsilon\otimes\beta_1\beta_1^{\mathrm{T}}), \\ \check{\Xi}_{12} =&-2(I\otimes\check{P}_6), \\ \check{\Xi}_{14} =&-(I\otimes\kappa_2AS^{\mathrm{T}})-\delta(L\otimes JS^{\mathrm{T}})-\delta(\Upsilon\otimes JS^{\mathrm{T}}), \\ \check{\Xi}_{15} =&-2(I\otimes\check{P}_7), \\ \check{\Xi}_{16} =&-(I\otimes S^{\mathrm{T}})-(I\otimes AS^{\mathrm{T}})+(I\otimes\check{P}_1), \\ \check{\Xi}_{17} =&(I\otimes BS^{\mathrm{T}})+\Theta_2(I\otimes\check{M}_1), \\ \check{\Xi}_{18} =&I\otimes CS^{\mathrm{T}}, \\ \check{\Xi}_{19} =&6(I\otimes\check{P}_6), \\ \check{\Xi}_{1,10} =&6(I\otimes\check{P}_7), \\ \check{\Xi}_{22} =&-(I\otimes\check{P}_3)-4(I\otimes\check{P}_6), \\ \check{\Xi}_{29} =&6(I\otimes\check{P}_6), \\ \check{\Xi}_{33} =&-(1-\lambda)(I\otimes\check{P}_2)-\Theta_1(I\otimes\check{M}_2) \\ &-\delta^2(L\otimes\kappa_2^2\beta_1\beta_1^{\mathrm{T}}), \\ \check{\Xi}_{34} =&-\delta(L\otimes\kappa_2JS^{\mathrm{T}})-\delta(\Upsilon\otimes\kappa_2JS^{\mathrm{T}}), \\ \check{\Xi}_{38} =&\Theta_2(I\otimes\check{M}_2), \\ \check{\Xi}_{44} =&-3(L\otimes S\beta_2\beta_2^{\mathrm{T}}S^{\mathrm{T}})-3(\Upsilon\otimes S\beta_2\beta_2^{\mathrm{T}}S^{\mathrm{T}}), \\ \check{\Xi}_{46} =&-(I\otimes\kappa_2S^{\mathrm{T}})-\delta(L\otimes\kappa_1JS^{\mathrm{T}}) \\ &-\delta(\Upsilon\otimes\kappa_1JS^{\mathrm{T}}), \\ \check{\Xi}_{47} =&I\otimes\kappa_1BS^{\mathrm{T}}, \\ \check{\Xi}_{48} =&I\otimes\kappa_2CS^{\mathrm{T}}, \\ \Xi_{55} =&-(I\otimes P_4)-4(I\otimes P_7), \\ \Xi_{5,10} =&6(I\otimes P_7), \\ \Xi_{66} =&\iota^2(I\otimes P_6)+\varrho^2(I\otimes P_7)-2(I\otimes S_2) \\ &-\delta^2(L\otimes S_2\beta_1\beta_1^{\mathrm{T}}S_2^{\mathrm{T}})-\delta^2(\Upsilon\otimes S_2\beta_1\beta_1^{\mathrm{T}}S_2^{\mathrm{T}}), \\ \check{\Xi}_{67} =&I\otimes\kappa_1BS^{\mathrm{T}}, \\ \check{\Xi}_{68} =&I\otimes\kappa_2CS^{\mathrm{T}}, \\ \check{\Xi}_{77} =&(I\otimes\check{P}_5)-(I\otimes\check{M}_1), \\ \check{\Xi}_{88} =&-(1-\lambda)(I\otimes\check{P}_5)-(I\otimes\check{M}_2), \\ \check{\Xi}_{99} =&-12(I\otimes\check{P}_6), \\ \check{\Xi}_{10,10} =&-12(I\otimes\check{P}_7), \end{aligned}$$

hold for

$$\check{\Xi}=[\check{\Xi}_{r\kappa}]<0,\ \text{where}\ r,\ \kappa=1,2,\cdots,10, \tag{21}$$

then the considered leader and followers are asymptotically synchronized under the proposed NFSDC scheme (6). In addition, the gain matrix J is given by $J=QS^{-1}$.

Proof We define $S_1=S^{-1}$, $S_2=\kappa_1S^{-1}$, $S_3=\kappa_2S^{-1}$, $Q=JS$, $\check{P}_{\mathfrak{K}}=SP_{\mathfrak{K}}S^{\mathrm{T}}$ ($\mathfrak{K}=1,2,\cdots,7$), $\check{M}_1=SM_1S^{\mathrm{T}}$, and $\check{M}_2=SM_2S^{\mathrm{T}}$. Then, both sides of LMI (8) are multiplied with $\mathrm{diag}(\underbrace{(I\otimes S),(I\otimes S),\cdots,(I\otimes S)}_{10\times})$ and $\check{\Xi}$ is as expressed in Theorem 1. If $\check{\Xi}<0$, in light of Eq. (21), we have $\dot{V}(t)<0$. This means that, based on the Lyapunov-Krosovskii stability theorem, it is established that the addressed MAS (1) with gain J is asymptotically synchronized. Thus, the proof is completed.

Remark 1 The above theorem ensures that the required criteria are obtained using some constructed inequalities and Lemma 1. It is observed that the integral portions which are less delay-dependent within the Writtinger inequality are ignored, and hence we achieve less conservativeness than Ma et al. (2016). Therefore, our results are more general than those in Ma et al. (2016).

Remark 2 Based on the derived LMI condition in Theorem 2, Algorithm 1 describes the calculation of the control gain matrix.

Algorithm 1 Asymptotic synchronization of MASs

Step 1: Set the parameters. A, B, and C are fixed system parameters. ι, β_1, and β_2 are selected as parameters, as well as some positive constants λ, δ, κ_1, κ_2, and ϱ-upper bound.

Step 2: Using Assumption 1, choose suitable matrices Θ_1 and Θ_2.

Step 3: There exist symmetric matrices $\check{P}_r > 0$ ($r = 1, 2, \cdots, 7$) and any matrix S such that LMIs (21) hold for a given upper bound.

Step 4: If the test is successful, the procedure proceeds to the next phase. Otherwise, return to steps 1 and 2 to change the parameters.

Step 5: The gain matrix is calculated by $J = QS^{-1}$.

Remark 3 If $\delta = 1$ and $\Delta J = 0$, then Eq. (5) is called nominally sampled data control. It is described as follows:

$$\begin{aligned} u_i(t) =& J\sum_{j=1}^{N} -l_{ij}(z_j(t-\varrho(t)) - z_i(t-\varrho(t))) \\ & - \phi_i\eta_i(t-\varrho(t)). \end{aligned} \tag{22}$$

From Remark 3, we readily arrive at the following corollary for considered synchronization error system (7) under SDC scheme (22):

Corollary 1 Under Assumption 1, for some positive constants ι, λ, ϱ, κ_1, and κ_2, if there exist positive matrices $\check{P}_{\mathfrak{K}}$ ($\mathfrak{K} = 1, 2, \cdots, 7$) and any matrix S with appropriate dimensions, such that the following equalities

$$\begin{aligned} \check{\Xi}_{11} =& (I\otimes\check{P}_2) + (I\otimes\check{P}_3) + (I\otimes\check{P}_4) - 4(I\otimes\check{P}_6) \\ & - 4(I\otimes\check{P}_7) - 2(I\otimes AS^{\mathrm{T}}) - \Theta_1(I\otimes\check{M}_1), \\ \check{\Xi}_{12} =& -2(I\otimes\check{P}_6), \\ \check{\Xi}_{14} =& -(L\otimes S^{\mathrm{T}}J) - (\Upsilon\otimes S^{\mathrm{T}}J), \\ \check{\Xi}_{15} =& -2(I\otimes\check{P}_7), \\ \check{\Xi}_{16} =& -(I\otimes S^{\mathrm{T}}) - (I\otimes AS^{\mathrm{T}}), \\ \check{\Xi}_{17} =& (I\otimes BS^{\mathrm{T}}) + \Theta_2(I\otimes\check{M}_1), \\ \check{\Xi}_{18} =& I\otimes CS^{\mathrm{T}}, \\ \check{\Xi}_{19} =& 6(I\otimes\check{P}_6), \\ \check{\Xi}_{1,10} =& 6(I\otimes\check{P}_7), \\ \check{\Xi}_{22} =& -(I\otimes\check{P}_3) - 4(I\otimes\check{P}_6),\ \check{\Xi}_{29} = 6(I\otimes\check{P}_6), \\ \check{\Xi}_{33} =& -(1-\lambda)(I\otimes\check{P}_2) - \Theta_1(I\otimes\check{M}_2), \\ \check{\Xi}_{38} =& \Theta_2(I\otimes\check{M}_2), \\ \check{\Xi}_{44} =& -(L\otimes\kappa_2JS^{\mathrm{T}}) - (\Upsilon\otimes\kappa_2JS^{\mathrm{T}}), \\ \check{\Xi}_{46} =& -(I\otimes\kappa_2S^{\mathrm{T}}) - (L\otimes\check{P}_1J) - (\Upsilon\otimes\check{P}_1J), \\ \check{\Xi}_{47} =& I\otimes\kappa_1BS^{\mathrm{T}}, \\ \check{\Xi}_{48} =& I\otimes\kappa_2BS^{\mathrm{T}}B, \\ \check{\Xi}_{55} =& -(I\otimes\check{P}_4) - 4(I\otimes\check{P}_7), \\ \check{\Xi}_{5,10} =& 6(I\otimes\check{P}_7), \\ \check{\Xi}_{66} =& \iota^2(I\otimes\check{P}_6) + \varrho^2(I\otimes\check{P}_7) - 2(I\otimes\kappa_1S^{\mathrm{T}}), \\ \check{\Xi}_{67} =& I\otimes\kappa_1BS^{\mathrm{T}}, \\ \check{\Xi}_{68} =& I\otimes\kappa_1CS^{\mathrm{T}}, \\ \check{\Xi}_{77} =& (I\otimes\check{P}_5) - (I\otimes\check{M}_1), \\ \check{\Xi}_{88} =& -(1-\lambda)(I\otimes\check{P}_5) - (I\otimes\check{M}_2), \\ \check{\Xi}_{99} =& -12(I\otimes\check{P}_6), \\ \check{\Xi}_{10,10} =& -12(I\otimes\check{P}_7), \end{aligned}$$

hold for

$$\check{\Xi} = [\check{\Xi}_{r\kappa}] < 0,\ \text{where } r, \kappa = 1, 2, \cdots, 10, \tag{23}$$

then the considered leader and followers are asymptotically synchronized under the proposed SDC scheme (6). In addition, the gain matrix J is given by $J = QS^{-1}$.

Proof The remaining elements are the same as those given in Theorem 2.

Remark 4 If there is no time-varying delay (i.e., $\iota(t) = 0$ in system (7)), then the multi-agent networks will be reconstructed as follows:

$$\dot{\eta}(t) = (I\otimes A)\eta(t) + (I\otimes B)h(\eta(t)) + U(t). \tag{24}$$

Now, using the same procedure as in Theorem 2, the following corollary can be obtained:

Corollary 2 Under Assumption 1, for some positive constants ϱ and κ_1, if there exist positive matrices $\check{P}_{\Re}$ ($\Re = 1, 2, 3$) and any matrix S with appropriate dimensions, such that the following equalities

$$\begin{aligned}
\check{\Xi}_{11} =&(I \otimes \check{P}_2) - 4(I \otimes \check{P}_3) - 2(I \otimes AS^{\mathrm{T}}) \\
&- \Theta_1(I \otimes \check{M}_1) - \delta^2(L \otimes \beta_1\beta_1^{\mathrm{T}}) \\
&- \delta^2(\Upsilon \otimes \beta_1\beta_1^{\mathrm{T}}), \\
\check{\Xi}_{12} =&-(I \otimes \kappa_1 AS^{\mathrm{T}}) - \delta(L \otimes JS^{\mathrm{T}}) \\
&- \delta(\Upsilon \otimes JS^{\mathrm{T}}), \\
\check{\Xi}_{13} =&-2(I \otimes \check{P}_3), \\
\check{\Xi}_{14} =&-(I \otimes S^{\mathrm{T}}) - (I \otimes AS^{\mathrm{T}}), \\
\check{\Xi}_{15} =&(I \otimes BS^{\mathrm{T}}) + \Theta_2(I \otimes \check{M}_1), \\
\check{\Xi}_{16} =&6(I \otimes \check{P}_3), \\
\check{\Xi}_{22} =&-2(L \otimes S\beta_2\beta_2^{\mathrm{T}}S^{\mathrm{T}}) - 2(\Upsilon \otimes S\beta_2\beta_2^{\mathrm{T}}S^{\mathrm{T}}), \\
\check{\Xi}_{24} =&-(I \otimes \kappa_2 S^{\mathrm{T}}) - \delta(L \otimes \kappa_1 JS^{\mathrm{T}}) \\
&- \delta(\Upsilon \otimes \kappa_1 JS^{\mathrm{T}}), \\
\check{\Xi}_{25} =&I \otimes B\kappa_1 S^{\mathrm{T}}, \\
\check{\Xi}_{33} =&-(I \otimes \check{P}_2) - \frac{4}{\varrho}(I \otimes \check{P}_3), \\
\check{\Xi}_{44} =&\varrho^2(I \otimes \check{P}_3) - 2(I \otimes \kappa_1 S^{\mathrm{T}}) \\
&- \delta^2(L \otimes \kappa_1^2\beta_1\beta_1^{\mathrm{T}}) - \delta^2(\Upsilon \otimes \kappa_1^2\beta_1\beta_1^{\mathrm{T}}), \\
\check{\Xi}_{45} =&I \otimes \kappa_1 BS^{\mathrm{T}}, \\
\check{\Xi}_{55} =&-(I \otimes \check{M}_1), \\
\check{\Xi}_{56} =&6(I \otimes \check{P}_3), \\
\check{\Xi}_{66} =&-12(I \otimes \check{P}_3),
\end{aligned}$$

hold for

$$\check{\Xi} = [\check{\Xi}_{r\kappa}] < 0, \ \text{ where } r, \ \kappa = 1, 2, ..., 6, \tag{25}$$

then MAS (24) can be asymptotically synchronized. In addition, the gain matrix J is given by $J = QS^{-1}$.

Proof We define $S_1 = S^{-1}$, $S_2 = \kappa_1 S^{-1}$, $Q = JS$, $\check{P}_{\Re} = SP_{\Re}S^{\mathrm{T}}$ ($\Re = 1, 2, 3$), and $\check{M}_1 = SM_1S^{\mathrm{T}}$. Then, both sides of LMI (25) are multiplied with $\mathrm{diag}(\underbrace{(I \otimes S), (I \otimes S), \cdots, (I \otimes S)}_{6\times})$, and $\check{\Xi}$ is as expressed in Theorem 2. If $\check{\Xi} < 0$, in light of LMI (25), we have $\dot{V}(t) < 0$. This means that, based on the Lyapunov-Krosovskii stability theorem, it is established that the addressed MAS (1) with gain J is asymptotically synchronized. Thus, the proof is completed.

Remark 5 In this paper, the synchronization problem is changed into the delay functional differential equation with error as its dynamics, and thus Lyapunov-Krosovskii stability is employed in the analysis. Note that the computational complexity depends on the number of sampling periods, the number of agents (N), and the state vector dimension of agent dynamics (n). If the number of agents, state vector dimension, and number of sampling periods increase, the computation for solving LMIs will be more complicated, which means that the size of the LMIs increases, and it is more time-consuming to verify the feasibility of the obtained LMI conditions. In this respect, all the results of the condition derived in this paper may be more suitable for small, low-dimensional networks of agents. For higher-order LMI approaches, deriving stable conditions in the maximum sampling period with high computational efficiency becomes future research work.

4 Numerical validation

The validation of the derived sufficient requirements has been carried out. Initial consideration is given to the MASs as a means of demonstrating the superiority of the proposed method over the existing methods. Next, in the context of a design example, the nonlinear NN model is studied.

4.1 Example 1: comparison example

Consider the MASs with time-varying delays similar to those in Ma et al. (2016) as follows:

$$\begin{cases}
\text{Leader:} \\
\dot{z}_0(t) = -Az_0(t) + Bg(z_0(t)) + Cg(z_0(t - \iota(t))), \\
\text{Followers:} \\
\dot{z}_i(t) = -Az_i(t) + Bg(z_i(t)) + Cg(z_i(t - \iota(t))) \\
\qquad\quad +U(t),
\end{cases} \tag{26}$$

where $i = 0, 1, 2, 3, 4$, and $g(z_i(t)) = \tanh(z_i(t))$ is an activation function. $\iota(t) = 0.79 \sin t + 1.11$ and

$$A = \begin{bmatrix} 1 & 0 \\ 0 & 1 \end{bmatrix}, \ B = \begin{bmatrix} 1 + \frac{\pi}{4} & 20 \\ 0.1 & 1 + \frac{\pi}{4} \end{bmatrix},$$

$$C = \begin{bmatrix} -1.3\sqrt{2}\frac{\pi}{4} & 0.1 \\ 0.1 & -1.3\sqrt{2}\frac{\pi}{4} \end{bmatrix}.$$

The leader's Laplacian and adjacency matrices associated with the MASs are

$$L=\begin{bmatrix}2&-1&0&-1\\0&1&-1&0\\-1&0&2&-1\\-1&0&-1&2\end{bmatrix},\Upsilon=\begin{bmatrix}1&0&0&0\\0&0&0&0\\0&0&0&0\\0&0&0&0\end{bmatrix}.$$

The constant parameters are $\iota=1.9$, $\lambda=0.79$, $\kappa_1=0.02$, $\kappa_1=0.04$, $\delta=0.7$, and $\varrho=0.079$. The other matrices are taken as

$$\beta_1=\begin{bmatrix}0.03&0\\0&0.04\end{bmatrix},\ \beta_2=\begin{bmatrix}0.02&0\\0&0.02\end{bmatrix}.$$

Employing the MATLAB LMI control toolbox, the gain matrix is calculated by solving LMIs (21) in Theorem 2. The corresponding gain matrix is

$$J=\begin{bmatrix}1.3326&0.4831\\0.1367&0.2541\end{bmatrix}.$$

In this scenario, the initial circumstances for the agent are chosen to be $z_0(0)=[0.8,-0.1]^{\mathrm{T}}$, $z_1(0)=[0.2,-0.6]^{\mathrm{T}}$, $z_2(0)=[0.4,-0.2]^{\mathrm{T}}$, $z_3(0)=[0.7,-0.3]^{\mathrm{T}}$, $z_4(0)=[0.6,-0.4]^{\mathrm{T}}$, and the network synchronization is shown in Fig. 1. The validity of Theorem 2 is confirmed by all supporters entering the area around the leader synchronization. The MAS state trajectories are shown in Fig. 2 and the synchronization of MASs with controllers is displaced in Fig. 3. The comparison of the time delay for system (7) is presented in Table 1. The corresponding control gain matrix and upper bound are presented in Table 2. The synchronization of MASs with different delays is displayed in Fig. 4.

4.2 Example 2: design example

The proposed units implemented in the NNs with two neurons are depicted in Figs. 5 and 6. System (24) can be expressed based on an analysis of the circuit nodes in Fig. 1. The values of the parameters given in Table 3 are taken from Lu (2002) and Wang TC et al. (2016), which are standards available in the existing works for the electronic circuits given in Figs. 5 and 6.

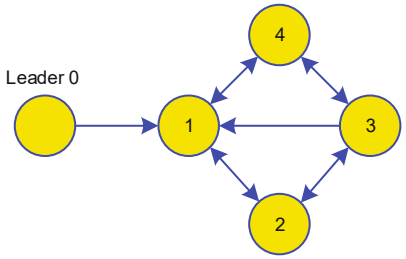

Fig. 1 Communication of MASs

Table 1 Comparison of the maximum allowable time delays

Method	ι
Ma et al. (2016)	1
Theorem 2	1.9
Corollary 1	1.7

Table 2 Upper bound ϱ and control gain matrix J corresponding to Example 1

Method	ϱ	J
Theorem 2	0.079	$\begin{bmatrix}1.3326&0.4831\\0.1367&0.2541\end{bmatrix}$
Corollary 1	0.044	$\begin{bmatrix}-1.2336&0.0875\\0.2390&-2.4249\end{bmatrix}$

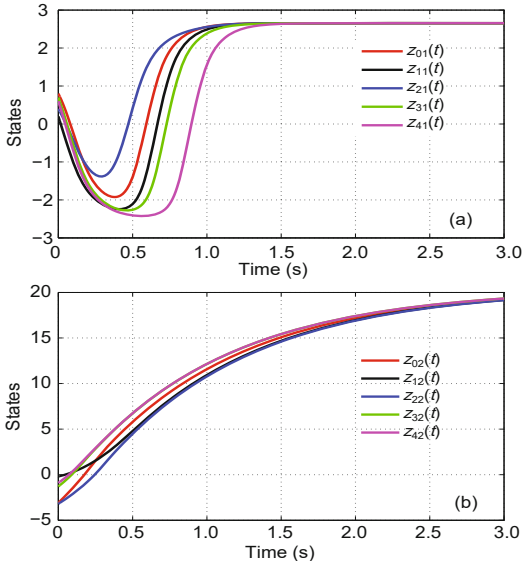

Fig. 2 Evolution of MASs $z_{i1}(t)$ (a) and $z_{i2}(t)$ (b) ($i=0,1,2,3,4$)

Table 3 Circuit parameters and their values

Parameter	Value	Parameter	Value
C_1, C_2	1 μF	R_{c11}	666 kΩ
R_1, R_2	1 MΩ	R_{c12}	10 MΩ
R_{b11}	500 kΩ	R_{c21}	5 MΩ
R_{b12}	10 MΩ	R_{b22}	Varies
R_{b21}	200 kΩ	R_{c22}	Varies

$$
\begin{cases}
\dfrac{\mathrm{d}z_1}{\mathrm{d}t} = -\dfrac{1}{C_1R_1}z_1(t) + \dfrac{1}{C_1R_{b11}}g(z_1(t)) \\
\quad + \dfrac{1}{C_1R_{b12}}g(z_2(t)) + \dfrac{1}{C_1R_{c11}}g(z_1(t-\iota(t))) \\
\quad + \dfrac{1}{C_1R_{c12}}g(z_2(t-\iota(t))), \\
\dfrac{\mathrm{d}z_2}{\mathrm{d}t} = -\dfrac{1}{C_2R_2}z_2(t) + \dfrac{1}{C_2R_{b21}}g(z_1(t)) \\
\quad + \dfrac{1}{C_2R_{b22}}g(z_2(t)) + \dfrac{1}{C_2R_{c21}}g(z_1(t-\iota(t))) \\
\quad + \dfrac{1}{C_2R_{c22}}g(z_2(t-\iota(t))).
\end{cases} \tag{27}
$$

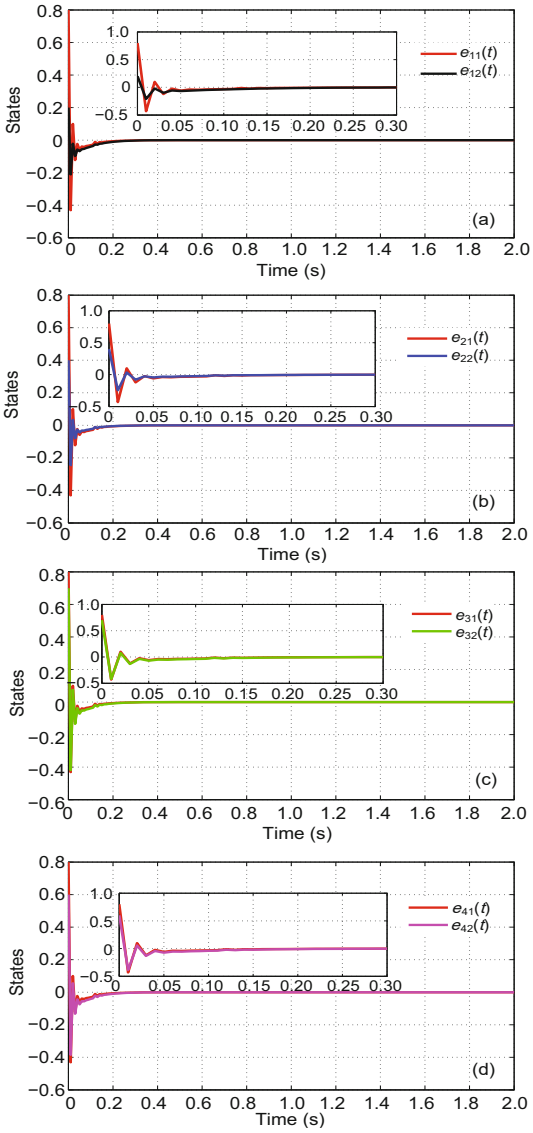

Fig. 3 Synchronization plots of errors $e_{1i}(t)$ (a), $e_{2i}(t)$ (b), $e_{3i}(t)$ (c), and $e_{4i}(t)$ (d) (i=1, 2) under non-fragile sampled data control

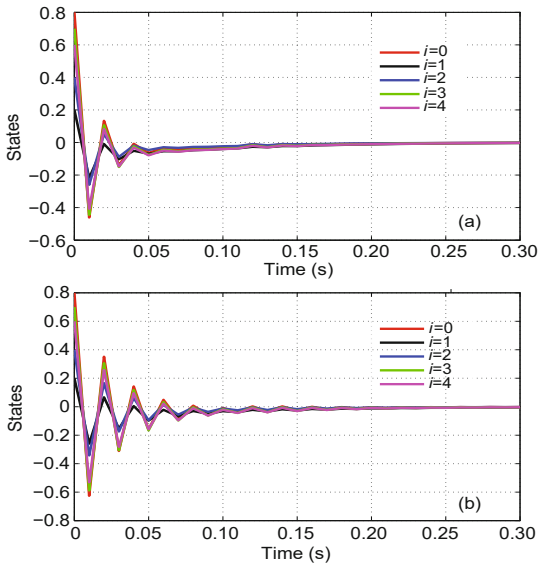

Fig. 4 Synchronization plots of errors $e_i(t)$ ($i = 0, 1, 2, 3, 4$) with $\iota = 1.2$ (a) or $\iota = 1.5$ (b)

Here, we consider an artificial circuit model based on Wang TC et al. (2016). The circuit has an activation function circuit with a time-varying delay and holds a corresponding unit. Each circuit unit contains inductors, resistors, capacitors, some operational amplifiers, and other common electrical components. The circuit implementations are adjusted according to the complexity of the NN model. In this investigation, NNs (27) have two neurons and can be rewritten as

$$
\dot{z}(t) = -Az(t) + Bg(z(t)) + Cg(z(t-\iota(t))), \tag{28}
$$

where $z(t) = [z_1(t),\ z_2(t)]^{\mathrm{T}} \in \mathbb{R}^n$.

Here, we look into the synchronization analysis of NFSDC in multi-agent networks using delayed NNs. Consider the leader and followers system (28) as follows:

$$
\begin{cases}
\text{Leader:} \\
\dot{z}_0(t) = -Az_0(t) + Bg(z_0(t)) + Cg(z_0(t-\iota(t))), \\
\text{Followers:} \\
\dot{z}_i(t) = -Az_i(t) + Bg(z_i(t)) + Cg(z_i(t-\iota(t))) \\
\qquad +U(t),
\end{cases} \tag{29}
$$

where $g(z_i(t)) = \tanh(z_i(t))$ ($i = 0, 1, 2, 3, 4$) are the activation functions, $\iota(t) = 0.69\sin t + 1.21$, and

$$
A = \begin{bmatrix} 1 & 0 \\ 0 & 1 \end{bmatrix},\ B = \begin{bmatrix} 2 & -0.1 \\ -0.5 & b_{22} \end{bmatrix},
$$

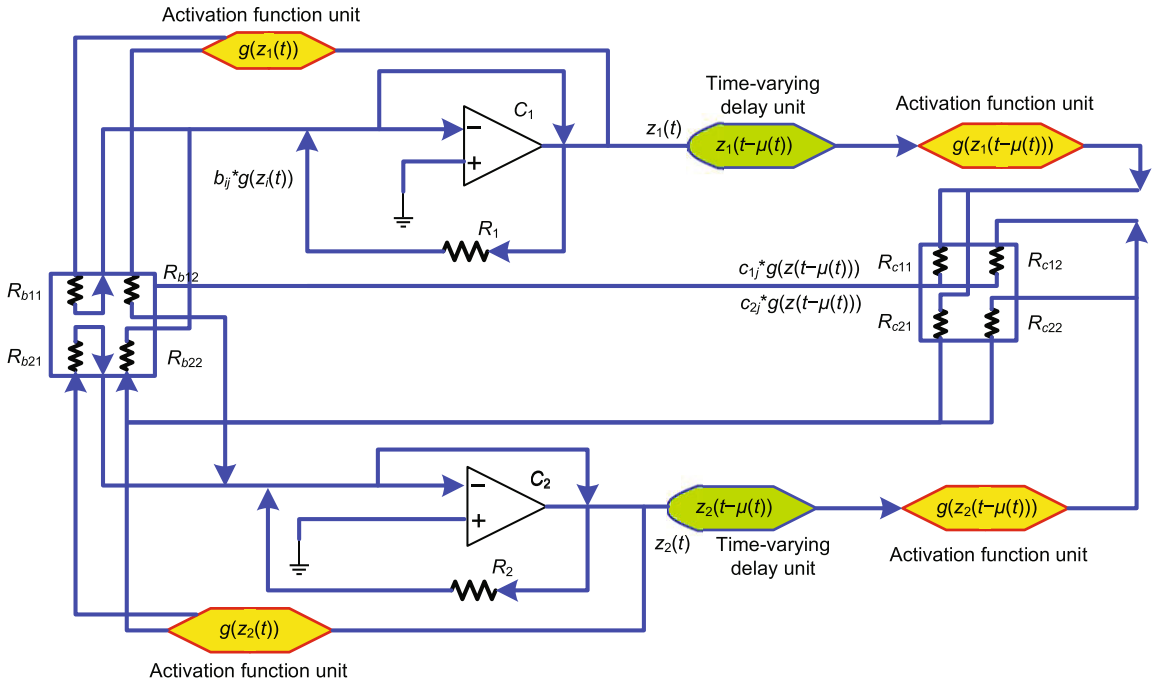

Fig. 5 Circuit realization of a two-dimensional neural network based circuit system with time-varying delays

$$C = \begin{bmatrix} -1.5 & -0.1 \\ -0.2 & c_{22} \end{bmatrix}.$$

It is permissible for b_{22} and c_{22} to be variable values, keeping $b_{22} + c_{22} = 0.5$.

The leader's Laplacian and adjacency matrices associated with the MASs are

$$L = \begin{bmatrix} 2 & -1 & 0 & -1 \\ 0 & 1 & -1 & 0 \\ -1 & 0 & 2 & -1 \\ -1 & 0 & -1 & 2 \end{bmatrix}, \Upsilon = \begin{bmatrix} 1 & 0 & 0 & 0 \\ 0 & 0 & 0 & 0 \\ 0 & 0 & 0 & 0 \\ 0 & 0 & 0 & 0 \end{bmatrix}.$$

Let us take constants $\iota = 1.9$, $\lambda = 0.69$, $\delta = 0.7$, $\kappa_1 = 0.01$, $\kappa_2 = 0.03$, and $\varrho = 0.084$. The matrices are

$$\beta_1 = \begin{bmatrix} 0.04 & 0 \\ 0 & 0.05 \end{bmatrix}, \beta_2 = \begin{bmatrix} 0.02 & 0 \\ 0 & 0.06 \end{bmatrix}.$$

Employing the MATLAB LMI control toolbox, the gain matrix is calculated by solving LMIs (21) in Theorem 2. The corresponding gain matrix is

$$J = \begin{bmatrix} 1.9542 & 1.3163 \\ 1.5364 & 2.8275 \end{bmatrix}.$$

For the present circumstances, the agents are chosen to be $z_0(0) = [1.4, -1.1]^{\mathrm{T}}$, $z_1(0) = [0.3, -0.6]^{\mathrm{T}}$, $z_2(0) = [0.2, -0.4]^{\mathrm{T}}$, $z_3(0) = [0.6, -0.2]^{\mathrm{T}}$, $z_4(0) = [0.5, -0.9]^{\mathrm{T}}$, and the network synchronization is plotted in Fig. 1. The validity of Theorem 2 is confirmed by all supporters entering the area around the leader synchronization. The state trajectories of MASs are shown in Fig. 7, and the synchronization of MASs with controllers is displaced in Fig. 8. The comparison of the maximum allowable time delay for system (5) is presented in Table 4. The corresponding upper bound and control gain matrix are presented in Table 5. The synchronization of MASs with different delays is displayed in Fig. 9.

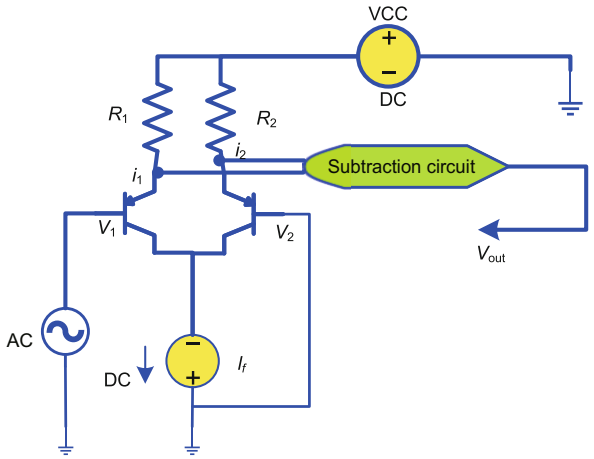

Fig. 6 Circuit realization of the tangent hyperbolic

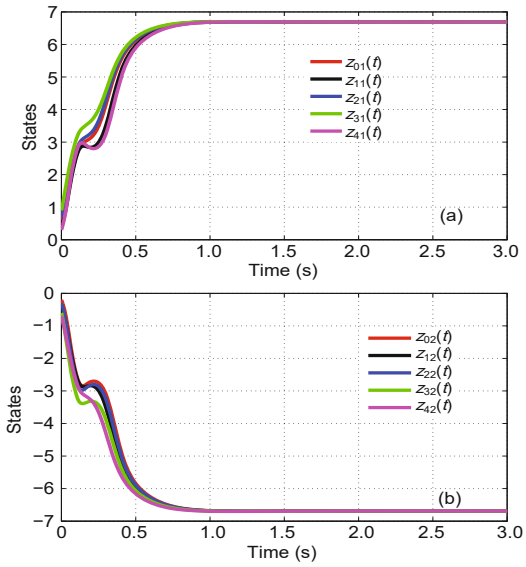

Fig. 7 Evolution of MASs $z_{i1}(t)$ (a) and $z_{i2}(t)$ (b) ($i=0,1,2,3,4$)

Table 4 Comparison of the maximum allowable time delays

Method	ι
Subramanian et al. (2019)	0.2
Ma et al. (2016)	1
Theorem 2	1.9
Corollary 2	1.5

Table 5 Upper bound ϱ and control gain matrix J corresponding to Example 2

Method	ϱ	J
Theorem 2	0.084	$\begin{bmatrix} 1.9542 & 1.3163 \\ 1.5364 & 2.8275 \end{bmatrix}$
Corollary 1	0.017	$\begin{bmatrix} 0.0327 & -1.1546 \\ 1.5810 & 0.4865 \end{bmatrix}$

5 Conclusions

In this work, the multi-agent system (MAS) synchronization problem has been investigated using a non-fragile sampled data control (NFSDC)

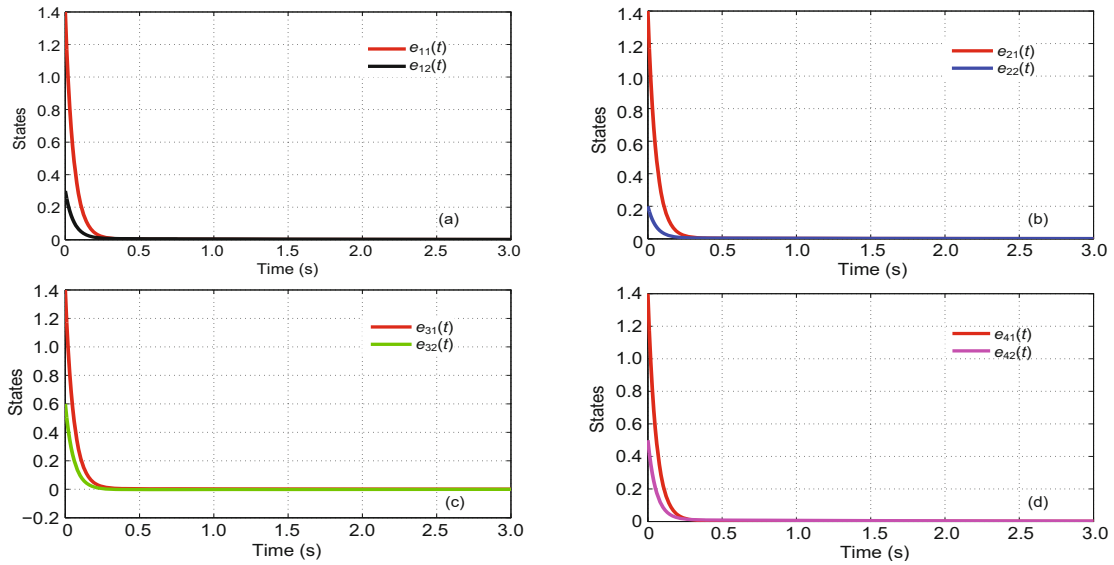

Fig. 8 Synchronization plots of errors $e_{1i}(t)$ (a), $e_{2i}(t)$ (b), $e_{3i}(t)$ (c), and $e_{4i}(t)$ (d) (i=1, 2) under non-fragile sampled data control

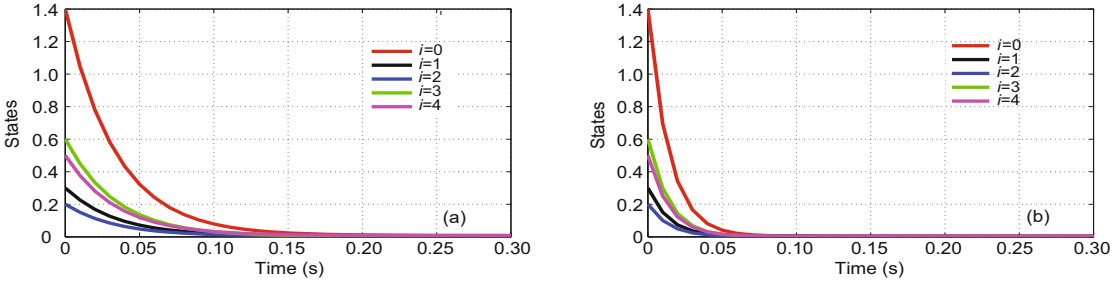

Fig. 9 Synchronization plots of errors $e_i(t)$ ($i=0,1,2,3,4$) with $\iota=1.4$ (a) or $\iota=1.7$ (b)

scheme. The suitable Lyapunov-Krosovskii functional has been constructed to derive the synchronization criteria for the proposed MASs, expressed in linear matrix inequality (LMI) forms. The proposed control scheme has achieved synchronization between the leader and follower systems with derived sufficient conditions. Finally, numerical validation has demonstrated the effectiveness of the presented method. As a future work topic, it will be exciting to explore the possibility of extending the NFSDC scheme to event-triggered control when unanticipated disruptions occur in MASs.

Peng et al. (2022) and Yang et al. (2022) discussed the event-triggered optimal control and observer-based fault detection filter methods. Zhu et al. (2022) discussed the novel reconstruction method for temperature distribution measurement based on ultrasonic tomography. Motivated by these studies, the proposed control method can be applied to multi-area nonlinear power systems based on the novel reconstruction approach, which will be considered in future work.

Contributors

Stephen AROCKIA SAMY designed the research. Raja RAMACHANDRAN drafted the paper. Yang CAO and Pratap ANBALAGAN revised and finalized the paper.

Compliance with ethics guidelines

Stephen AROCKIA SAMY, Raja RAMACHANDRAN, Pratap ANBALAGAN, and Yang CAO declare that they have no conflict of interest.

Data availability

Due to the nature of this research, participants of this study did not agree for their data to be shared publicly, so supporting data are not available.

References

Ali MS, Agalya R, Saroha S, et al., 2020a. Leaderless consensus of non-linear mixed delay multi-agent systems with random packet losses via sampled-data control. *Int J Contr Autom Syst*, 18(7):1885-1893. https://doi.org/10.1007/s12555-019-0446-1

Ali MS, Agalya R, Shekher V, et al., 2020b. Non-fragile sampled data control for stabilization of non-linear multi-agent system with additive time varying delays, Markovian jump and uncertain parameters. *Nonl Anal Hybr Syst*, 36:100830. https://doi.org/10.1016/j.nahs.2019.100830

Alimi AM, Aouiti C, Assali AE, 2019. Finite-time and fixed-time synchronization of a class of inertial neural networks with multi-proportional delays and its application to secure communication. *Neurocomputing*, 332:29-43. https://doi.org/10.1016/j.neucom.2018.11.020

Beard RW, McLain TW, Goodrich MA, et al., 2002. Coordinated target assignment and intercept for unmanned air vehicles. *IEEE Trans Robot Autom*, 18(6):911-922. https://doi.org/10.1109/TRA.2002.805653

Chen LN, Aihara K, 1995. Chaotic simulated annealing by a neural network model with transient chaos. *Neur Netw*, 8(6):915-930. https://doi.org/10.1016/0893-6080(95)00033-V

Fax JA, Murray RM, 2004. Information flow and cooperative control of vehicle formations. *IEEE Trans Autom Contr*, 49(9):1465-1476. https://doi.org/10.1109/TAC.2004.834433

Jia Q, Tang WKS, Halang WA, 2011. Leader following of nonlinear agents with switching connective network and coupling delay. *IEEE Trans Circ Syst I Reg Papers*, 58(10):2508-2519. https://doi.org/10.1109/TCSI.2011.2131230

Jia Q, Han ZY, Tang WKS, 2019. Synchronization of multi-agent systems with time-varying control and delayed communications. *IEEE Trans Circ Syst I Reg Papers*, 66(11):4429-4438. https://doi.org/10.1109/TCSI.2019.2928040

Jiang XL, Xia GH, Feng ZG, et al., 2020. Non-fragile H_∞ consensus tracking of nonlinear multi-agent systems with switching topologies and transmission delay via sampled-data control. *Inform Sci*, 509:210-226. https://doi.org/10.1016/j.ins.2019.08.078

Kaviarasan B, Kwon OM, Park MJ, et al., 2021. Stochastic faulty estimator-based non-fragile tracking controller for multi-agent systems with communication delay. *Appl Math Comput*, 392:125704. https://doi.org/10.1016/j.amc.2020.125704

Lavanya S, Nagarani S, 2022. Leader-following consensus of multi-agent systems with sampled-data control and looped functionals. *Math Comput Simul*, 191:120-133. https://doi.org/10.1016/j.matcom.2021.08.002

Liu JL, Yin TT, Yue D, et al., 2021. Event-based secure leader-following consensus control for multiagent systems with multiple cyber attacks. *IEEE Trans Cybern*, 51(1):162-173. https://doi.org/10.1109/TCYB.2020.2970556

Liu Y, Tong LY, Lou JG, et al., 2019. Sampled-data control for the synchronization of Boolean control networks. *IEEE Trans Cybern*, 49(2):726-732. https://doi.org/10.1109/TCYB.2017.2779781

Lu HT, 2002. Chaotic attractors in delayed neural networks. *Phys Lett A*, 298(2-3):109-116. https://doi.org/10.1016/S0375-9601(02)00538-8

Ma TD, Lewis FL, Song YD, 2016. Exponential synchronization of nonlinear multi-agent systems with time delays and impulsive disturbances. *Int J Rob Nonl Contr*, 26(8):1615-1631. https://doi.org/10.1002/rnc.3370

Meng ZY, Ren W, Cao YC, et al., 2011. Leaderless and leader-following consensus with communication and input delays under a directed network topology. *IEEE Trans Syst Man Cybern B Cybern*, 41(1):75-88. https://doi.org/10.1109/TSMCB.2010.2045891

Peng ZN, Luo R, Hu JP, et al., 2022. Distributed optimal tracking control of discrete-time multiagent systems via event-triggered reinforcement learning. *IEEE Trans Circ Syst I Reg Papers*, 69(6):3689-3700. https://doi.org/10.1109/TCSI.2022.3177407

Rakkiyappan R, Kaviarasan B, Cao JD, 2015. Leader-following consensus of multi-agent systems via sampled-data control with randomly missing data. *Neurocomputing*, 161:132-147. https://doi.org/10.1016/j.neucom.2015.02.056

Ren W, Sorensen N, 2008. Distributed coordination architecture for multi-robot formation control. *Robot Auton Syst*, 56(4):324-333. https://doi.org/10.1016/j.robot.2007.08.005

Sang H, Zhao J, 2019. Exponential synchronization and L_2-gain analysis of delayed chaotic neural networks via intermittent control with actuator saturation. *IEEE Trans Neur Netw Learn Syst*, 30(12):3722-3734. https://doi.org/10.1109/TNNLS.2019.2896162

Saravanakumar R, Mukaidani H, Amini A, 2020. Non-fragile exponential consensus of nonlinear multi-agent systems via sampled-data control. *IFAC-PapersOnLine*, 53(2):5677-5682. https://doi.org/10.1016/j.ifacol.2020.12.1591

Seuret A, Gouaisbaut F, 2013. Wirtinger-based integral inequality: application to time-delay systems. *Automatica*, 49(9):2860-2866. https://doi.org/10.1016/j.automatica.2013.05.030

Sompolinsky H, Crisanti A, Sommers HJ, 1988. Chaos in random neural networks. *Phys Rev Lett*, 61(3):259-262. https://doi.org/10.1103/PhysRevLett.61.259

Subramanian K, Muthukumar P, Joo YH, 2019. Leader-following consensus of nonlinear multi-agent systems via reliable control with time-varying communication delay. *Int J Contr Autom Syst*, 17(2):298-306. https://doi.org/10.1007/s12555-018-0323-3

Tan XG, Cao JD, Li XD, 2019. Consensus of leader-following multiagent systems: a distributed event-triggered impulsive control strategy. *IEEE Trans Cybern*, 49(3):792-801. https://doi.org/10.1109/TCYB.2017.2786474

Tang Y, Gao HJ, Zhang WB, et al., 2015. Leader-following consensus of a class of stochastic delayed multi-agent systems with partial mixed impulses. *Automatica*, 53:346-354. https://doi.org/10.1016/j.automatica.2015.01.008

Wang CY, Zuo ZY, Qi ZQ, et al., 2019. Predictor-based extended-state-observer design for consensus of MASs with delays and disturbances. *IEEE Trans Cybern*, 49(4):1259-1269. https://doi.org/10.1109/TCYB.2018.2799798

Wang TC, He X, Huang TW, 2016. Complex dynamical behavior of neural networks in circuit implementation. *Neurocomputing*, 190:95-106. https://doi.org/10.1016/j.neucom.2016.01.030

Wang WP, Jia X, Luo X, et al., 2019. Fixed-time synchronization control of memristive MAM neural networks with mixed delays and application in chaotic secure communication. *Chaos Sol Fract*, 126:85-96. https://doi.org/10.1016/j.chaos.2019.05.041

Wang YL, Cao JD, Hu JQ, 2014. Pinning consensus for multi-agent systems with non-linear dynamics and time-varying delay under directed switching topology. *IET Contr Theory Appl*, 8(17):1931-1939. https://doi.org/10.1049/iet-cta.2014.0032

Xu XY, Li WQ, Wang MQ, 2021. Distributed output tracking of nonlinear multi-agent systems by linear sampled-data control. *Neurocomputing*, 462:238-246. https://doi.org/10.1016/j.neucom.2021.07.060

Yang J, Zhong QS, Shi KB, et al., 2022. Co-design of observer-based fault detection filter and dynamic event-triggered controller for wind power system under dual alterable DoS attacks. *IEEE Trans Inform Forens Secur*, 17:1270-1284. https://doi.org/10.1109/TIFS.2022.3160355

Yue DD, Cao JD, Li Q, et al., 2021. Neural-network-based fully distributed adaptive consensus for a class of uncertain multiagent systems. *IEEE Trans Neur Netw Learn Syst*, 32(7):2965-2977. https://doi.org/10.1109/TNNLS.2020.3009098

Zhang D, Xu ZH, Karimi HR, et al., 2018. Distributed H_∞ output-feedback control for consensus of heterogeneous linear multiagent systems with aperiodic sampled-data communications. *IEEE Trans Ind Electron*, 65(5):4145-4155. https://doi.org/10.1109/TIE.2017.2772196

Zhao C, Liu XZ, Zhong SM, et al., 2021. Leader-following consensus of multi-agent systems via novel sampled-data event-triggered control. *Appl Math Comput*, 395:125850. https://doi.org/10.1016/j.amc.2020.125850

Zhao YS, Li XD, Duan PY, 2019. Observer-based sliding mode control for synchronization of delayed chaotic neural networks with unknown disturbance. *Neur Netw*, 117:268-273. https://doi.org/10.1016/j.neunet.2019.05.013

Zheng MW, Li LX, Peng HP, et al., 2017. Finite-time stability analysis for neutral-type neural networks with hybrid time-varying delays without using Lyapunov method. *Neurocomputing*, 238:67-75. https://doi.org/10.1016/j.neucom.2017.01.037

Zhong QS, Yang J, Shi KB, et al., 2022. Event-triggered H_∞ load frequency control for multi-area nonlinear power systems based on non-fragile proportional integral control strategy. *IEEE Trans Intell Transp Syst*, 23(8):12191-12201. https://doi.org/10.1109/TITS.2021.3110759

Zhou B, Liao XF, Huang TW, et al., 2015. Leader-following exponential consensus of general linear multi-agent systems via event-triggered control with combinational measurements. *Appl Math Lett*, 40:35-39. https://doi.org/10.1016/j.aml.2014.09.009

Zhu B, Zhong QS, Chen YS, et al., 2022. A novel reconstruction method for temperature distribution measurement based on ultrasonic tomography. *IEEE Trans Ultras Ferroelectr Freq Contr*, 69(7):2352-2370. https://doi.org/10.1109/TUFFC.2022.3177469